

Article

Transcriptomic Analysis Provides Insights into Microplastic and Heavy Metal Challenges in the Line Seahorse (*Hippocampus erectus*)

Ying Liu ¹, Dongwei Shang ^{1,2}, Yanjing Yang ¹, Pei Cui ¹ and Jinhui Sun ^{1,*} 

¹ Key Laboratory of Aquatic Ecology and Aquaculture of Tianjin, College of Fisheries, Tianjin Agricultural University, Tianjin 300384, China

² Tianjin Nongken Bohai Agricultural Group Co., Ltd., Tianjin 301809, China

* Correspondence: jhsun1008@163.com

Abstract: Microplastics (MPs) are ubiquitous pollutants that have potentially harmful and toxic effects. MPs are frequently ingested by aquatic animals, as microplastics share a similar size and color to their food. Heavy metals are harmful and difficult to degrade, have a wide range of sources and an extended residual time from exposure to recovery. Although the effects of MPs and heavy metals on the performance of aquatic species have been extensively studied, the molecular mechanisms of MP and heavy metal (Pb, Cd and Cu) exposure on aquatic organisms remain unclear. Here, the effects of MPs and heavy metal accumulation on the line seahorse, *Hippocampus erectus*, were investigated at the molecular level using transcriptome analysis. Using gene ontology (GO) and Kyoto Encyclopedia of Genes and Genomes (KEGG) enrichment analyses, we found that immune, metabolic, and apoptotic pathways were affected in the heavy metal group, whereas the DNA damage repair and metabolism pathways were mainly involved in the MP group. Both types of stress caused significant changes in the genes related to the antioxidant pathway in *H. erectus* larvae. Transcriptome differences between the treatment groups were analyzed, and sensitive candidate genes (*Hsp70*, *Hsp90*, *Sod*, etc.) were screened. The response characteristics of seahorses to MP environmental stress were also investigated. Using seahorse as a biological model and candidate sensitive genes as a basis, our results provide a theoretical basis for detecting MPs and heavy metals pollution in coastal areas.

Keywords: seahorse; heavy metals; microplastics; transcriptomics



Citation: Liu, Y.; Shang, D.; Yang, Y.; Cui, P.; Sun, J. Transcriptomic Analysis Provides Insights into Microplastic and Heavy Metal Challenges in the Line Seahorse (*Hippocampus erectus*). *Fishes* **2022**, *7*, 338. <https://doi.org/10.3390/fishes7060338>

Academic Editors: Teresa Bottari and Monique Mancuso

Received: 4 October 2022

Accepted: 12 November 2022

Published: 18 November 2022

Publisher's Note: MDPI stays neutral with regard to jurisdictional claims in published maps and institutional affiliations.



Copyright: © 2022 by the authors. Licensee MDPI, Basel, Switzerland. This article is an open access article distributed under the terms and conditions of the Creative Commons Attribution (CC BY) license (<https://creativecommons.org/licenses/by/4.0/>).

1. Introduction

Plastic pollution in the ocean is among the most important global environmental problems. Plastics are widely used in manufacturing and everyday life, owing to their durability, water resistance, light weight, and inexpensive cost [1]. Since the first production of plastic in 1907, plastic production has increased approximately 200 fold. In 2019, global plastic production reached 368 million tons [2]. Hence, a large amount of plastic waste is released into the marine environment. Because plastics are non-degradable, they are usually broken down into smaller particles by biotic and abiotic factors [3].

Microplastics (MPs), plastic granules of less than 5 mm in size [4,5], are widely distributed in the ocean and readily ingested by marine organisms [6]. Aquatic organisms can directly or indirectly ingest MPs and accumulate them in the food chain [7,8]. MPs have been found in different trophic levels, from invertebrates to vertebrates [9,10]. The intake of MPs can affect the feeding rate, digestion rate, and behavior of organisms [11]. Excessive accumulation leads to metabolic disorders, oxidative stress, immune damage, and even genetic changes, thereby leading to biological growth retardation [12]. Therefore, it is particularly important to study the pollution, toxicity, migration, metabolism, safety, and ecological risks of MPs in marine environments.

In environmental waters, MPs do not exist alone. Because they are hydrophobic, they can be used as ‘carriers’ for toxic pollutants [13] such as heavy metals [14,15] and persistent organic pollutants [16,17] that can accumulate in organisms. Heavy metals are harmful and difficult to degrade and have a wide range of sources and an extended residual time from exposure and recovery [18,19]. Moreover, heavy metals have strong accumulation characteristics, thereby directly or indirectly threatening human health [20,21]. Owing to increasingly serious marine pollution, it is important to study the harmful effects of heavy metal pollution on marine organisms. Many studies have reported that heavy metals accumulate in various marine fishes. Edem et al. [22] studied the accumulation of heavy metals in the various tissues of Nile tilapia (*Oreochromis niloticus*). Upon reaching a certain level, heavy metal accumulation caused lesions in the main organs and tissues of the fish, eventually leading to their death. Duran et al. [23] detected heavy metals content in the muscles of 11 commercial fish species in Turkey and evaluated their food safety and pollution status. Furthermore, the effects of heavy metals and MPs on the physiological responses of aquatic species have been investigated. However, few studies have evaluated the effects of combined exposure of heavy metals and MPs on the immune and metabolic aspects of aquatic organisms, especially on their molecular mechanisms.

Recent advances in DNA sequencing and omics technologies have promoted the study of biological mechanisms. High-throughput RNA-seq technology enables the comprehensive analysis of differentially expressed genes (DEGs) under different treatments to improve the understanding of the entire transcriptome of an organism [24]. RNA-seq has been widely used in various fields of aquatic biology, and white shrimp [25], zebrafish [26], oysters [27], and holothurians [28] have been studied. The liver is one of the most important metabolic organs of fish and plays an important role in regulating immune defense and hormone synthesis in fishes [29]. Liu et al. [30] studied grass carp (*Ctenopharyngodon idella*) exposed to MPs for 21 days and performed transcriptome sequencing of the livers; they identified 1554 annotated DEGs. Gene ontology (GO) and the Kyoto Encyclopedia of Genes and Genomes (KEGG) pathway enrichment analyses further identified important pathways, such as those involved in energy and lipid metabolism. In addition, heavy metals in marine environments can enter aquatic animals through the food chain and gradually accumulate [31]. The accumulation of heavy metals not only has a strong toxic effect on marine aquatic organisms, but also directly threatens food quality and safety through enrichment. Therefore, heavy metal accumulation has received considerable research attention worldwide.

The lined seahorse *Hippocampus erectus*, is a small marine teleost fish belonging to the same order, family, and genus as the sea dragon. It mainly feeds on live organisms such as small crustaceans and newly hatched fish larvae. Seahorses are valuable aquatic organisms that have medicinal, food, and ornamental purposes. At least 46 species of seahorses have been identified worldwide [32]. Previous studies on seahorses have mostly focused on the effects of single pollutants, and there have been a few studies on the toxic mechanisms of combined pollutants. Complex interactions between pollutants may trigger different biochemical pathways and toxicological reactions in organisms [33,34]. In particular, the effect of the coexistence of MPs and heavy metals on organisms requires further investigation.

Thus, this study was aimed at investigating the effects of marine plastics and heavy metal exposure. Transcriptome analysis revealed the effects of the accumulation of MPs and heavy metals on *H. erectus* via molecular mechanisms. In addition, transcriptome differences between the treatment groups and the related molecular mechanisms were analyzed. Biomarkers under the stress of environmental pollutants were screened to provide a basis for the healthy breeding and quality control of seahorses. The response characteristics of seahorses to MP environmental stress were also described.

2. Materials and Methods

2.1. Experimental Materials

The seahorse used in this experiment was *H. erectus*, which was obtained from the Tianjin Hangu salt farm (Tianjin, China). Healthy seahorses with a length of 7.20 ± 0.49 cm and weight of 1.70 ± 0.35 g were selected. After transportation to the laboratory, they were briefly cultured in an indoor recirculating aquaculture system for seven days. The seawater was sand-filtered with a salinity range of 24–26‰, temperature of 25 ± 1 °C, and a dissolved oxygen concentration of >5 mg/L.

The high-density polyethylene (HDPE) MP standard was produced by Sinopec Maoming Petrochemical Company (Tianjin, China). White, uneven powder particles (particle size range: 15–80 µm) were observed. HDPE (1 g) was uniformly dispersed in water, and 10^4 MP particles per gram were observed by microscope. Seahorse feed was comprised of frozen mysid shrimp (Tianjin, China). The mysid shrimp culture was captured in the pond, frozen in $50 \times 30 \times 5$ cm block of ice, and wrapped in a nylon bag stored at -20 °C.

2.2. Experimental Design

A total of 135 seahorses of similar size and weight were selected, equally divided into three groups ($n = 45$), and housed in 60 L glass breeding aquarium containers. Three replicates were set up for each group, that is, 15 seahorse larvae were placed in each experimental tank. The treatment groups were as follows: the HM-group was the heavy metal + MPs group and fed with mysid shrimp containing heavy metals (Pb, Cd and Cu, Sinopharm Chemical Reagent Co. LTD, Tianjin, China) and MPs; the MP-group was the MPs group fed a diet containing only MPs without heavy metals, and the number of MPs on the bait was 1600/g; the Control group was fed with frozen mysid shrimp without heavy metals and MPs.

The diets were prepared as previously described [35]. Details of the feed preparation method are summarized in Supplementary Table S1. Briefly, MP particles were placed into a 4 L glass aquarium tank and the tank was aerated for even distribution. A heavy metal solution comprising 0.05 mg/L lead, 0.01 mg/L cadmium, and 0.05 mg/L copper was added, and the heavy metal ions were adsorbed onto MPs via aeration. The concentrations of the heavy metals were determined using inductively coupled plasma mass spectrometry (ICP-MS). MPs containing saturated heavy metal ions were centrifuged, collected, and mixed with the mysid shrimp. MPs containing heavy metal ions were adsorbed onto the mysid shrimp. The same method was used to prepare the MP diet without heavy metal ions. The control group was fed only mysid shrimp (no pollution). Fresh feed was prepared before each feeding.

Daily management of the experiment was as follows: seahorses were fed approximately 10% of the total weight of the farmed seahorses twice a day at 9:00 a.m. and 15:00 p.m. After feeding for 2 h, the residual feed was removed using the siphon method. On day 45 of the culture experiment, 6 seahorse juvenile were randomly selected from each treatment group for transcriptome analysis. The livers of the juveniles were removed with sterilized scissors and tweezers, immediately placed in a CMO tube, frozen in liquid nitrogen, and stored in a freezer at -80 °C until further analysis.

2.3. Total RNA Extraction from Liver

RNA extraction was performed as described by Brown et al. [36]. Briefly, on an ultra-clean bench, total RNA was extracted using a universal RNA kit (Accurate Biotechnology Co., Ltd., Shenzhen, China) according to the manufacturer's instructions. Frozen liver samples were homogenized and added with chloroform and isopropanol for separation and purification. RNA concentration and quality were determined using a K5500 spectrophotometer (Caio, Beijing, China) and 1% agarose gel electrophoresis.

2.4. cDNA Synthesis

The PrimerScript™ RT reagent Kit with gDNA Eraser (Takara, Dalian, China) was used according to the manufacturer's instructions. First, genomic DNA was extracted. The reverse transcript reaction (reaction system; Table S1) was performed at 42 °C for 2 min (Tables S2 and S3). The synthesized cDNA samples were stored at −20 °C.

2.5. Transcription Library and Sequencing

A NEBNext® Ultra™ RNA library preparation kit (NEB, Ipswich, MA, USA) was used to construct the sequencing libraries. Transcriptome high-throughput sequencing was performed on the Illumina platform, and the sequencing strategy was PE150 (Annuoyouda Gene Technology (Beijing) Co., Ltd. Beijing, China).

Perl scripts [37] were used to process raw data to ensure the quality, and the filter conditions were as follows: (1) reads with junction contamination (the number of bases in reads that were junction contaminated was >5 bp); (2) low-quality reads (the bases with mass value $Q < 19$ accounted for 50% of the total bases in reads); and (3) reads containing >5% N.

2.6. Transcriptome Assembly and Annotation

The resulting transcripts and unigenes were evaluated using Trinity software (v2.4.0; Trinity Release, CA, USA) [38]. Bowtie2 (version 2.2.3) was used to compare the assembled sequences with the assembled transcript sequences. The read ratio of the above sequence was compared for rate analysis, and uniformity was analyzed using a Python script. BUSCO (Benchmarking Universal Single-Copy Orthologs) obtained standard non-redundant homologous gene information from the OrthoDB database, and BLAST (NCBI) [39], HMMER-SCAN (v3.2.1), and other methods were used to evaluate the integrity of the transcriptome assembly data.

TransDecoder (version 3.0.1) [40] predicted the open reading frame (ORF), and Trino-tate annotates the predicted ORFS.

2.7. Transcriptome Differential Expression Analysis

RSEM software (v1.1.17) [41,42] was used to calculate the expression levels of genes or transcripts, and DEGseq software (v1.18.0) [43] was used to analyze DEGs. Genes with $Q \leq 0.05$ and $|\log_2 \text{ratio}| \geq 1$ were selected as DEGs.

2.8. GO and KEGG Analysis

GO and KEGG metabolism pathways were analyzed. The Goatools (v0.5.7) software (<https://github.com/tanghaibao/Goatools> accessed on 1 November 2022) were used to determine highly enriched GO terms in genes, and KOBAS 3.0 (<http://kobas.cbi.pku.edu.cn/annotate/> accessed on 1 November 2022) for significantly enriched KEGG pathways.

2.9. Real-Time Fluorescent Quantitative PCR Analysis

Ten DEGs were selected to verify the RNA-Seq results. According to the unigene sequence in the transcriptome library, specific primers (Table 1) were designed using the Primer Premier 5 software (<http://www.premierbiosoft.com> accessed on 1 November 2022).

β 2-Microglobulin ($\beta 2m$) was used as the internal reference gene. The relative expression level of each gene was calculated according to Livak et al. [44], and the relative expression level of the target gene was calculated using the $2^{-\Delta\Delta C_t}$ method. TB Green Premix Ex Taq™ II (TaKaRa, Japan) was used for quantitative expression analysis in the Eppendorf realplex4. There were nine seahorse larvae in each group, and three seahorse livers were mixed in a sample with three replicates.

Table 1. Genes used in RT-qPCR and their primer sequences.

Gene Name	Primer Sequences (5'-3')	Amplification Efficiencies
<i>XRCC2</i>	F: CCGCCAAAGTGTTCGTGA R: TGATCCAAATGCGCCATG	99
<i>Sod</i>	F: TCACATACTTCACGGGTTTCG R: AGGGAAATGTTCAAGGTACTGC	102
<i>Hsp70</i>	F: GTCGGTGAAATAACAGGGAACA R: CTCTGGGTCTACAGGTATTAAGGTG	95
<i>Stard7</i>	F: CGTTTGGCTCCTTTTGTGC R: GCGGGTTTGTCTACTCCTCTG	97
<i>Cyp51a1</i>	F: CGCCTGGTTGGGTTTCTT R: TCAAACAACGCTCCAACAGG	102
<i>Fadsd6</i>	F: TGGTGCTTGTACTACTACCTTCG R: CTTGATGCTTCTCGTGGTCG	104
<i>Apoa4</i>	F: CGTCTTCGTTTTGGCTGTTT R: TCTTTTCCGAGATCCGACTGT	103
<i>Akt3</i>	F: GCGACGGAGAAGTTGTTGAG R: GTTGTC AAGGAAGGATGGGTC	96
<i>Il-10</i>	F: GGAGGACACGAGGGACTTGA R: GCCTTTGTTTTGCATCTGACTG	100
<i>Aif1</i>	F: ACGCCATCAATGAGGCCTTTT R: TCTTGGCAAGTCCCAGTTTCT	102
<i>B2m</i>	F: TACACCCACCAGCCAGGAAA R: GGACTCGACGACATCGAACATC	100

2.10. Statistical Analysis

FDR < 0.001 and $|\log_2 \text{ratio}| \geq 1$ were used as the thresholds to determine significant differences in gene expression. Data obtained from the experiments were analyzed using SPSS statistical software and are expressed as the mean \pm standard deviation. Significant differences were measured using analysis of variance and Duncan's multiple comparison method. Statistical significance was set at $p < 0.05$.

3. Results

3.1. Sequencing Results

After high-throughput sequencing (Table S4), the Control group, HM-group and MP-group obtained 49,556,386, 49,404,042, and 48,043,100 raw reads, respectively. After filtration, 47,880,348 (Control group), 47,987,534 (HM- group), and 46,520,778 (MP-group) clean reads were obtained. The clean Q30 base rate (%) represents the proportion of bases with a mass value > 30 (error rate < 0.1%) in the filtered total sequence, which is an indicators of data reliability. Q30 values were >94%, indicating that the data were reliable.

3.2. Transcriptome Assembly Results

According to Table S5, high-throughput DNA sequencing data generated 86,712 transcripts, with a length of 200–1000 bp, an average length of 1,443,25 bp, and an N50 length of 2485 bp. After further assembly, 42,264 single gene clusters were obtained, with an average length of 1,122.71 bp and N50 of 2223 bp. Among them, unigenes in the range of 200–600, 600–1000, 1000–2000, and >2000 bp accounted for 53.3%, 12.4%, 16.3%, and 18.0%, respectively.

According to Table S6, the proportion of unigenes annotated in the Nr database was the highest, reaching 53.6%. The unigenes annotated by the Nt database accounted for 44.5%; 19,506 unigenes were annotated in the GO database, accounting for 46.2%; the KO database annotated the least number of unigenes (12,046).

3.3. GO and KOG Statistics

Using the annotation results of Trinotate, the genes annotated in each GO entry were counted, and statistical results were obtained according to the secondary GO entry

(Figure 1). The main category of biological processes was cellular processes, accounting for 74.7%, followed by biological regulation and metabolic processes, accounting for 56.7% and 49.7%, respectively. The most important categories in the molecular functional categories were binding function (72.9%) and catalytic activity (35.3%). The representative categories of cell components were cell parts (87.3%), organelles (57.2%), and organelle parts (45.4%). In the KOG database, 15 454 genes were annotated into 25 orthologous groups (Figure 2). Among them, signal transduction mechanisms (T, 21.3%) and general function prediction (R, 21.1%) represented the largest group, followed by post-translational modification/protein turnover/molecular chaperones (O, 8.3%).

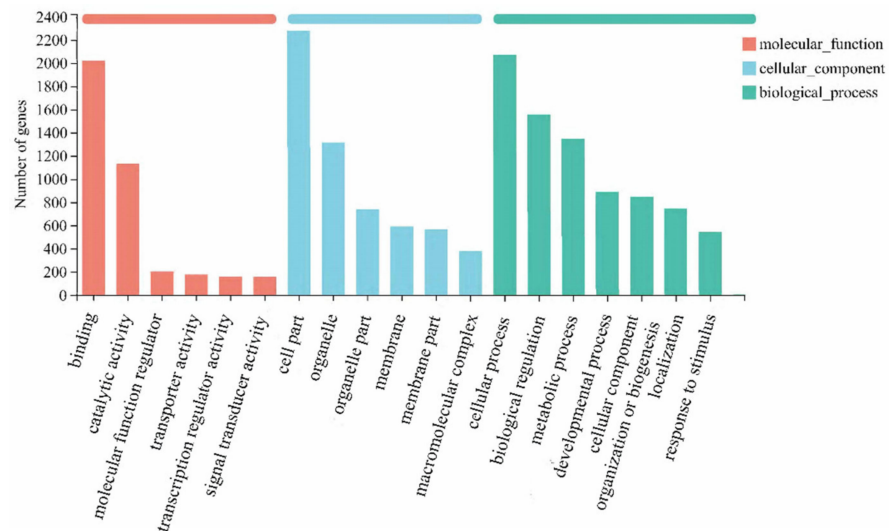


Figure 1. GO statistics histogram.

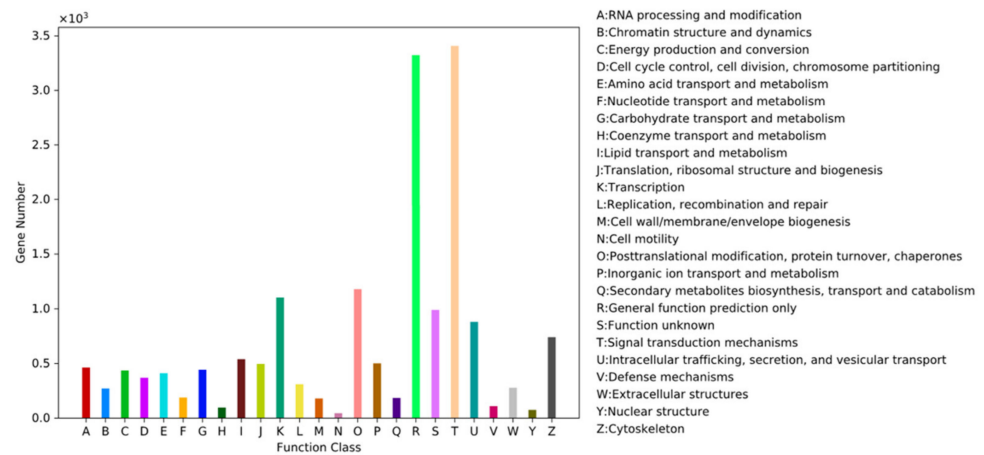


Figure 2. KOG chart of Functioned gene dives.

3.4. DEGs

After comparing the HM-group with the Control group, 14,009 DEGs were obtained (Figure 3), of which 5543 were significantly upregulated and 8466 were significantly downregulated. A total of 20,030 DEGs (14,016 were significantly upregulated and 6014 were significantly downregulated) were obtained by comparing the MP-group with the Control group. The number of upregulated genes in the heavy metal A group was lower than that of the downregulated genes, whereas the number of upregulated genes in the MP-group accounted for the majority. As shown in Figure 4, there were 2851 DEGs in the three groups after pairwise comparison. There were 7324 DEGs between the HM-group vs the Control group and the MP-group vs the Control group, whereas only 6685 DEGs were significantly

expressed between the HM-group vs the Control group, and 12,706 DEGs were significantly different expressed in the MP group vs the Control group.

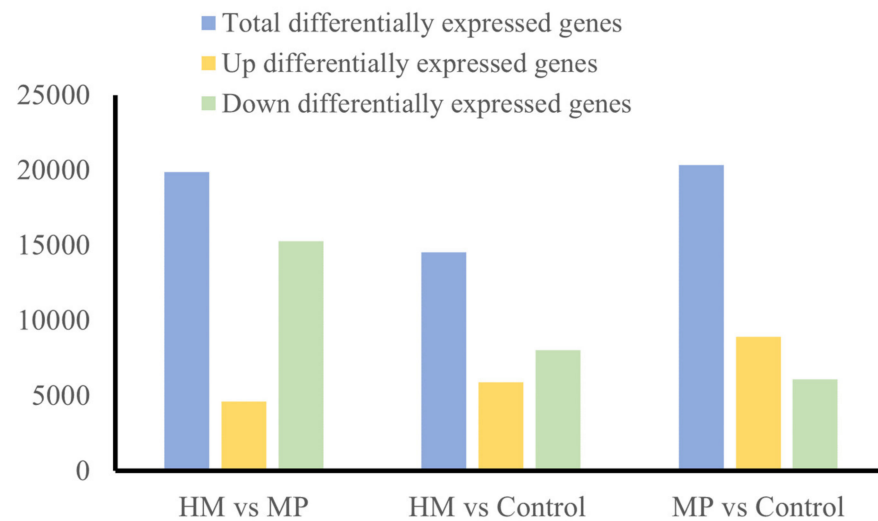


Figure 3. Differentially expressed genes in the liver transcriptome of *H. erectus*.

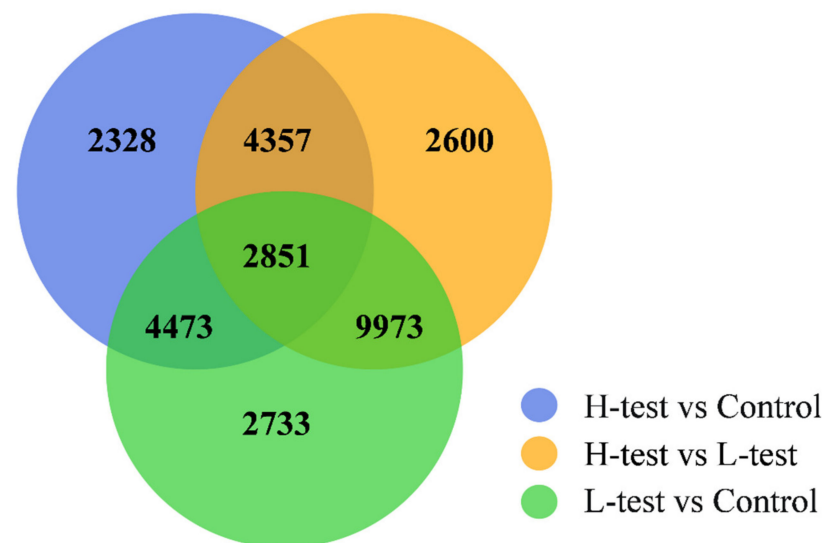


Figure 4. Venn diagram of differentially expressed gene in the liver transcriptome of *H. erectus*.

3.5. KEGG Enrichment Analysis

The differentially expressed genes between the HM-group and the Control group were enriched in 332 pathways. The significantly enriched pathways included protein digestion and absorption, steroid biosynthesis, and ECM–receptor interaction. The differentially expressed genes in the MP-group and the Control group were enriched in 332 pathways, and the significantly enriched pathways included homologous recombination and DNA replication.

Tables 2 and 3 list the top 20 KEGG enriched metabolic pathways. Among them, immune pathways (such as ECM–receptor interaction, IgA intestinal immune network, Legionella disease, and PI3K–Akt signaling pathway), metabolic pathways (such as protein digestion and absorption, steroid biosynthesis, fat digestion and absorption, and glyceride metabolism), and apoptosis (iron-dependent programmed cell death) were affected in the HM-group. The significantly expressed genes mainly included superoxide dismutase (*SOD*), heat shock protein 70 (*Hsp70*), heat shock protein 90 (*Hsp90*), phosphatidylinositol 3-kinase regulatory subunit (*Pik3r1*), cytochrome C (*Cytc*), caspase-9 (*Casp9*), caspase-3

(*Casp3*), cyclin-dependent kinase inhibitor (*P21*), RAC- γ serine/threonine-protein kinase (*Akt3*), interleukin 10 (*IL-10*), Toll-like receptor 2 (*Tlr2*), and chemokine receptor 9 (*Ccr9*).

Table 2. Top 20 KEGG metabolic pathways of HM-group vs. differential control genes.

Pathway ID	Upregulated DEGs	Downregulated DEGs	Q Value	Metabolic Pathway Annotation
map04974	23	45	4.9×10^{-3}	Protein digestion and absorption
map00100	3	13	5.9×10^{-3}	Steroid biosynthesis
map04512	22	44	1.23×10^{-2}	ECM-receptor interaction
map04923	9	31	7.38×10^{-2}	Regulation of lipolysis in adipocytes
map04975	20	5	1.947×10^{-1}	Fat digestion and absorption
map00561	17	19	1.947×10^{-1}	Glycerolipid metabolism
map04672	7	8	1.947×10^{-1}	Intestinal immune network for IgA Production
map05134	21	4	1.947×10^{-1}	Legionellosis
map05145	31	23	1.947×10^{-1}	Toxoplasmosis
map04978	12	9	2.153×10^{-1}	Mineral absorption
map04151	62	81	2.153×10^{-1}	PI3K-Akt signaling pathway
map04930	6	24	2.153×10^{-1}	Type II diabetes mellitus
map00604	6	5	2.153×10^{-1}	Glycosphingolipid biosynthesis—ganglio series
map00830	11	8	2.153×10^{-1}	Retinol metabolism
map04721	17	19	2.153×10^{-1}	Synaptic vesicle cycle
map02010	18	16	2.802×10^{-1}	ABC transporters
map00520	23	5	2.802×10^{-1}	Amino sugar and nucleotide sugar metabolism
map05414	27	24	3.534×10^{-1}	Dilated cardiomyopathy
map04612	19	1	6.349×10^{-1}	Antigen processing and presentation
map04216	18	4	6.349×10^{-1}	Ferroptosis

Table 3. Top 20 KEGG metabolic pathways for MP-group vs control enrichment.

Pathway ID	Upregulated DEGs	Downregulated DEGs	Q Value	Metabolic Pathway Annotation
map03440	39	1	2.7×10^{-3}	Homologous recombination
map03030	34	0	9.2×10^{-3}	DNA replication
map00590	27	6	2.594×10^{-1}	Arachidonic acid metabolism
map04110	92	2	2.594×10^{-1}	Cell cycle
map03460	40	4	2.594×10^{-1}	Fanconi anemia pathway
map04724	80	32	2.594×10^{-1}	Glutamatergic synapse
map00480	33	3	2.594×10^{-1}	Glutathione metabolism
map00240	62	9	2.594×10^{-1}	Pyrimidine metabolism
map04977	25	4	2.594×10^{-1}	Vitamin digestion and absorption
map03420	32	0	2.685×10^{-1}	Nucleotide excision repair
map00520	35	4	5.093×10^{-1}	Amino sugar and nucleotide sugar metabolism
map03410	25	1	5.093×10^{-1}	Base excision repair
map00010	44	6	5.093×10^{-1}	Glycolysis/Gluconeogenesis
map00340	11	7	5.093×10^{-1}	Histidine metabolism
map03430	15	0	5.093×10^{-1}	Mismatch repair
map04114	80	12	5.093×10^{-1}	Oocyte meiosis
map03050	28	0	5.093×10^{-1}	Proteasome
map00230	113	14	5.093×10^{-1}	Purine metabolism
map04742	24	12	5.093×10^{-1}	Taste transduction
map05414	59	15	5.416×10^{-1}	Dilated cardiomyopathy

The MP-group should include enrichment for DNA damage repair (such as homologous recombination, DNA replication, cell cycle, nucleotide excision repair, and base excision repair) and metabolism (arachidonic acid metabolism, glutathione metabolism, and glycolysis). It was found that *SOD*, *Hsp70*, *Hsp90*, *P21*, *P53* (tumor protein P53), *Bcl-2*-

related X protein (*Bax*), STAR-related lipid transfer domain protein 7 (*Stard7*), apolipoprotein A-IV (*Apoa4*), lanosterol 14 α -demethylase (*Cyp51*), Δ -6 fatty acyl desaturase (*Fadsd6*), DNA mismatch repair protein MSH3 (*Msh3*), DNA damage binding protein DDB2 (*Ddb2*), DNA repair protein XRCC2 (*Xrcc2*), DNA repair protein RAD52 (*Rad52*), 8-oxoguanine glycosylation enzyme (*Ogg1*), mismatch repair endonuclease PMS2 (*Pms2*), and other genes play an important role in the physical stress caused by MPs.

3.6. Real-Time Fluorescent Quantitative PCR Results

To verify the accuracy of the RNA-Seq results, 10 differentially expressed genes (Table 1) were selected for validation. Using β 2m as the internal reference gene, the differences in transcription patterns of these 10 genes in the experimental and treatment groups were detected by RT-qPCR analysis (Figure 5a). The results of the RT-qPCR analysis were compared with those of the transcriptome analysis. The results paralleled those of transcriptomics, and the trend of relative expression level was consistent with that of RNA-seq (Figure 5b), confirming that the results of the transcriptome analysis were reliable.

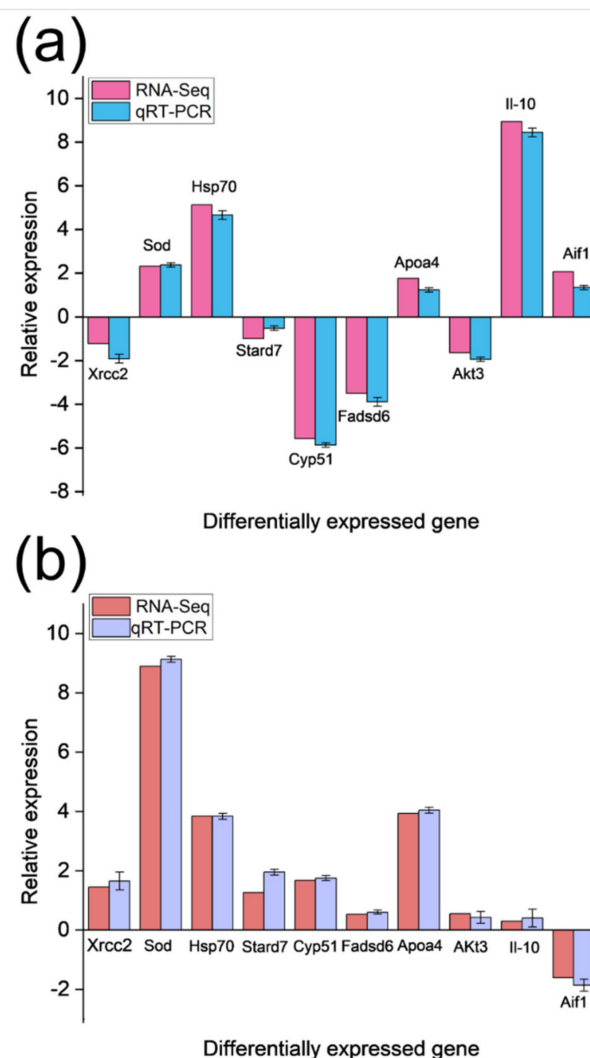


Figure 5. Comparative analysis of RT-qPCR and RNA-Seq results in HM-group (a) and MP-group (b).

4. Discussion

Drastic changes in environmental conditions greatly affect the growth, development, and feeding of aquatic organisms [45,46]. Stress due to environmental pollutants also affects physiological activities, such as the growth and development of aquatic organisms.

In this study, we analyzed the transcriptomic changes in the liver of juvenile lined seahorses under heavy metal stress. Compared with the Control group, 14,009 and 20,030 genes were differentially expressed in the heavy metal group, indicating that heavy metal stress may activate various cellular metabolic pathways in response to the toxic physiological stress effects on the lined seahorse. Heavy metal stress caused significant changes in the expression of genes related to antioxidants and apoptosis, including *SOD*, *Hsp70*, *Hsp90*, *Cyts*, *Casp9*, *Casp3*, *P21*, *P53*, and *Bax*, and significantly altered the expression of *Pik3r1*, *P21*, *Akt3*, *Il-10*, *Tlr*, and other genes in the immune pathway. Meanwhile, a total of 20,030 differentially expressed genes were obtained in the MP-group compared with the control group (14,016 differentially expressed genes were significantly up-regulated and 6014 differentially expressed genes were significantly down-regulated). MPs stress significantly affected the expression of genes related to fatty acid synthesis and DNA damage repair, such as *Stard7*, *Apoa4*, *Cyp51*, *Fadsd6*, *Msh3*, *Ddb2*, *Xrcc2*, *Rad52*, *Ogg1*, and *Pms2*. The number of upregulated genes due to MP stress (Figure 5) was 2.6 times that of heavy metal stress, indicating that MP stress affected more genes, which may be related to the ability of *H. erectus* larvae to resist physical damage.

Heavy metal and MPs stress can increase the reactive oxygen species (ROS) content in aquatic organisms. ROS accumulation partly stimulates the body's resistance and infection response [47,48]. In this study, both stress treatments resulted in the significant upregulation of antioxidant-related genes, such as *Hsp70*, *Hsp90*, and *SOD*, possibly to eliminate excessive ROS, whereas heat shock proteins (HSPs) act as molecular chaperones to prevent the aggregation of harmful proteins, promote protein folding, and help repair damaged proteins [49,50].

We found that the significantly upregulated genes under heavy metal stress were mainly *P21*, *Cyts*, *Casp9*, and *Casp3*, whereas the differentially expressed apoptosis-related genes in the MP stress group were *p53*, *P21*, and *Bax*. A large release of cytochrome C activates caspase-9, which in turn activates caspase-3 and induces apoptosis [51]. P53 is involved in a variety of DNA damage-repair pathways, such as chromatin remodeling and base excision repair [52]. P21 is a cyclin-dependent kinase inhibitor located downstream of the P53 gene. Its main role is to reduce the replication and accumulation of damaged DNA and inhibit apoptosis [53]. Bax affects apoptosis via an antioxidant mechanism [54]. Our results showed that heavy metal stress activated the caspase-dependent apoptosis pathway, whereas MP stress caused the upregulation of genes related to the inhibition of apoptosis and activated many DNA damage repair genes to resist physical damage [49].

The PI3K-Akt signaling pathway regulates important processes, such as apoptosis, protein synthesis, and the cell cycle, in organisms upon exposure to an environmental stimulus or cytotoxic damage [55]. Our results showed that the expression of genes related to the PI3K-Akt signaling pathway was significantly affected by heavy metal stress, with 62 and 81 upregulated and downregulated genes, respectively. The expression of two key genes, *Pik3r1* and *Akt3*, in this pathway was significantly downregulated. Under MP stress, the PI3K-Akt signaling pathway was not significantly affected. In a study on *Haliotis diversicolor*, Sun et al. [56] found that the expression of *Pi3k* and *Akt3* genes was significantly downregulated during stress, hypoxia, or a pathogen attack. In addition, the differential genes involved in immunity in this pathway, such as *IL-10* and *Tlr*, were significantly upregulated, whereas *Ccr9* was downregulated. *IL-10* can downregulate the expression of T helper cytokines (Th1 and Th2) and chemokines and is a key regulator of immunity and inflammation [57,58]. The Tlr signaling pathway also plays a key role in innate immune defense mechanisms [59,60]. These results indicate that chemical stress, rather than physical stress, is more likely to lead to immune system disorders in lined seahorses, which may eventually result in increased disease frequency.

We found that genes related to fatty acid metabolism under MP stress, such as *Fadsd6*, *Apoa4*, *Stard7*, and *Cyp51*, were significantly upregulated, whereas only *Apoa4* was significantly upregulated in the heavy metal stress group. Fatty acid metabolism in fishes is sensitive to physical damage [61,62]. STAR is a rate-limiting protein that mainly mediates

mitochondrial transport during cholesterol biosynthesis [63]. CYP51 is a key enzyme in sterol biosynthesis and is the most evolutionarily conserved member of the CYP superfamily [64]. In this study, MP stress led to the upregulation of genes related to steroids and unsaturated fatty acids, whereas heavy metal stress led to the opposite trend, probably because fatty acids play an important role in the resistance of seahorses to physical damage stress.

Related studies have shown that changes in environmental conditions can disrupt the balance between oxidation and antioxidant systems of the body, resulting in DNA damage. Protein chaperones, cell cycle regulation, DNA repair, and other processes often reduce DNA damage [65]. In this study, multiple DNA damage repair pathways, such as homologous recombination, nucleotide excision repair, DNA replication, cell cycle, mismatch repair, pyrimidine metabolism, and base excision repair, were enriched under MP stress. The upregulated genes identified were *Msh3*, *Ddb2*, *Xrcc2*, *Rad52*, *Ogg1*, and *Pms2*. Among these genes, only *Pms2* was significantly upregulated under heavy metal stress, indicating that physical stress was more likely to cause DNA damage in seahorses and the organism resisted the damage caused by external heavy metal stress by inducing the overexpression of repair genes.

5. Conclusions

In this study, the Control group, HM-group, and MP-groups were cultured for 45 days, and transcriptome of the liver was sequenced using analysis. After sequencing the data assembly, 22,513 unigenes were obtained. GO and KEGG enrichment analyses revealed that the immune, metabolic, and apoptotic pathways were affected in the heavy metal group, whereas DNA damage repair and metabolism were mainly involved in the MP group. Both types of stress caused significant changes in genes related to the antioxidant pathway (*Hsp70*, *Hsp90*, and *SOD*) in lined seahorse larvae. Moreover, the transcriptome differences between the treatment groups were analyzed to screen for sensitive candidate genes that could be used to monitor heavy metal contamination during artificial breeding of *H. erectus* and detect changes in heavy metal concentrations in the marine environment.

Supplementary Materials: The following supporting information can be downloaded at: <https://www.mdpi.com/article/10.3390/fishes7060338/s1>, Table S1: Reaction system conditions for genomic DNA removal; Table S2: Reverse transcription reaction system; Table S3: Reverse transcription PCR program; Table S4: Summary of the sequencing data of *H. erectus*; Table S5: Assembly results; Table S6: Summary of comments in each database.

Author Contributions: J.S.: conceptualization, supervision, writing—review and editing, and funding acquisition. Y.L.: formal analysis, visualization, conceptualization, software, data curation, writing—original draft. D.S.: investigation, methodology, writing—review, and editing. Y.Y. and P.C.: resources and visualization. All authors have read and agreed to the published version of the manuscript.

Funding: This work was supported by the National Key Research and Development Program of China (Grant No. 2018YFD0900206) and the Tianjin Science and Technology Program Project (21YDTPJC00340).

Institutional Review Board Statement: The study was conducted according to the guidelines of the Declaration of Helsinki and approved by the Institutional Review Board of the Animal Protection and Utilization Committee of Tianjin Agricultural University, in accordance with the provisions and guidelines established by the Committee. All animal experiments were conducted in accordance with the guidelines and approval of the Animal Research and Ethics Committees of the Chinese Academy of Sciences (SCSIO-IACUC-2019-000137).

Data Availability Statement: The data presented in this study are available on request from the corresponding author.

Conflicts of Interest: The authors declare no conflict of interest.

References

1. Wang, S.; Huang, H.; Liu, C.; Xia, Y.; Ye, C.; Luo, Z.; Cai, C.; Wang, C.; Lyu, L.; Bi, H.; et al. Waterproof and Breathable Graphene-Based Electronic Fabric for Wearable Sensors. *Adv. Mater. Technol.* **2022**, *7*, 2200149. [[CrossRef](#)]
2. Welden, N.A.; Lusher, A.L. Impacts of changing ocean circulation on the distribution of marine microplastic litter. *Integr. Environ. Assess. Manag.* **2017**, *13*, 483–487. [[CrossRef](#)] [[PubMed](#)]
3. Cózar, A.; Echevarría, F.; González-Gordillo, J.I.; Irigoien, X.; Úbeda, B.; Hernández-León, S.; Palma, Á.T.; Navarro, S.; García-De-Lomas, J.; Ruiz, A.; et al. Plastic debris in the open ocean. *Proc. Natl. Acad. Sci. USA* **2014**, *111*, 10239–10244. [[CrossRef](#)] [[PubMed](#)]
4. Lebreton, L.; Slat, B.; Ferrari, F.; Sainte-Rose, B.; Aitken, J.; Marthouse, R.; Hajbane, S.; Cunsolo, S.; Schwarz, A.; Levivier, A.; et al. Evidence that the Great Pacific Garbage Patch is rapidly accumulating plastic. *Sci. Rep.* **2018**, *8*, 1–15. [[CrossRef](#)] [[PubMed](#)]
5. Cole, M.; Lindeque, P.; Halsband, C.; Galloway, T.S. Microplastics as contaminants in the marine environment: A review. *Mar. Pollut. Bull.* **2011**, *62*, 2588–2597. [[CrossRef](#)] [[PubMed](#)]
6. Setälä, O.; Fleming-Lehtinen, V.; Lehtiniemi, M. Ingestion and transfer of microplastics in the planktonic food web. *Environ. Pollut.* **2014**, *185*, 77–83. [[CrossRef](#)] [[PubMed](#)]
7. Chen, G.; Li, Y.; Wang, J. Occurrence and ecological impact of microplastics in aquaculture ecosystems. *Chemosphere* **2021**, *274*, 129989. [[CrossRef](#)]
8. Athey, S.N.; Albotra, S.D.; Gordon, C.A.; Monteleone, B.; Seaton, P.; Andrady, A.L.; Taylor, A.R.; Brander, S.M. Trophic transfer of microplastics in an estuarine food chain and the effects of a sorbed legacy pollutant. *Limnol. Oceanogr. Lett.* **2020**, *5*, 154–162. [[CrossRef](#)]
9. Guzzetti, E.; Sureda, A.; Tejada, S.; Faggio, C. Microplastic in marine organism: Environmental and toxicological effects. *Environ. Toxicol. Pharmacol.* **2018**, *64*, 164–171. [[CrossRef](#)]
10. Da Costa Araújo, A.P.; De Andrade Vieira, J.E.; Malafaia, G. Toxicity and trophic transfer of polyethylene microplastics from *Poecilia reticulata* to *Danio rerio*. *Sci. Total Environ.* **2020**, *742*, 140217. [[CrossRef](#)]
11. Jiang, W.; Fang, J.; Du, M.; Gao, Y.; Fang, J.; Jiang, Z. Microplastics influence physiological processes, growth and reproduction in the Manila clam, *Ruditapes philippinarum*. *Environ. Pollut.* **2021**, *293*, 118502. [[CrossRef](#)] [[PubMed](#)]
12. Benson, N.U.; Agboola, O.D.; Fred-Ahmadu, O.H.; De-la-Torre, G.E.; Oluwalana, A.; Williams, A.B. Micro (nano) plastics prevalence, food web interactions and toxicity assessment in aquatic organisms: A review. *Front. Mar. Sci.* **2022**, *291*, 851281. [[CrossRef](#)]
13. Caruso, G. Microplastics as vectors of contaminants. *Mar. Pollut. Bull.* **2019**, *146*, 921–924. [[CrossRef](#)] [[PubMed](#)]
14. Brennecke, D.; Duarte, B.; Paiva, F.; Caçador, I.; Canning-Clode, J. Microplastics as vector for heavy metal contamination from the marine environment. *Estuar. Coast. Shelf Sci.* **2016**, *178*, 189–195. [[CrossRef](#)]
15. Liu, S.; Huang, J.; Zhang, W.; Shi, L.; Yi, K.; Yu, H.; Zhang, C.; Li, S.; Li, J. Microplastics as a vehicle of heavy metals in aquatic environments: A review of adsorption factors, mechanisms, and biological effects. *J. Environ. Manag.* **2021**, *302*, 113995. [[CrossRef](#)]
16. Kinigopoulou, V.; Pashalidis, I.; Kalderis, D.; Anastopoulos, I. Microplastics as carriers of inorganic and organic contaminants in the environment: A review of recent progress. *J. Mol. Liq.* **2022**, *350*, 118580. [[CrossRef](#)]
17. Patrício-Rodrigues, J.; Duarte, A.C.; Santos-Echeandía, J.; Rocha-Santos, T. Significance of interactions between microplastics and POPs in the marine environment: A critical overview. *TrAc Trends Anal. Chem.* **2019**, *111*, 252–260. [[CrossRef](#)]
18. El Bahgy, H.E.; Elabd, H.; Elkorashey, R.M. Heavy metals bioaccumulation in marine cultured fish and its probabilistic health hazard. *Environ. Sci. Pollut. Res.* **2021**, *28*, 41431–41438. [[CrossRef](#)]
19. Zamora-Ledezma, C.; Negrete-Bolagay, D.; Figueroa, F.; Zamora-Ledezma, E.; Ni, M.; Alexis, F.; Guerrero, V.H. Heavy metal water pollution: A fresh look about hazards, novel and conventional remediation methods. *Environ. Technol. Innov.* **2021**, *22*, 101504. [[CrossRef](#)]
20. Steinhäuser, S.L.; Agyeman, N.; Turrero, P.; Ardura, A.; Garcia-Vazquez, E. Heavy metals in fish nearby electronic waste may threaten consumer's health. Examples from Accra, Ghana. *Mar. Pollut. Bull.* **2022**, *175*, 113162. [[CrossRef](#)]
21. Renu, K.; Chakraborty, R.; Myakala, H.; Koti, R.; Famurewa, A.C.; Madhyastha, H.; Vellingiri, B.; George, A.; Gopalakrishnan, A.V. Molecular mechanism of heavy metals (Lead, Chromium, Arsenic, Mercury, Nickel and Cadmium)-induced hepatotoxicity—A review. *Chemosphere* **2021**, *271*, 129735. [[CrossRef](#)] [[PubMed](#)]
22. Edem, C.A.; Vincent, O.; Grace, I.; Rebecca, E.; Joseph, E. Distribution of heavy metals in bones, gills, livers and muscles of (*Tilapia*) *Oreochromis niloticus* from Henshaw Town Beach market in Calabar Nigeria. *Pak. J. Nutr.* **2009**, *8*, 1209–1211.
23. Duran, A.; Tuzen, M.; Soylak, M. Assessment of trace metal concentrations in muscle tissue of certain commercially available fish species from Kayseri, Turkey. *Environ. Monit. Assess.* **2014**, *186*, 4619–4628. [[CrossRef](#)] [[PubMed](#)]
24. Martin, S.A.; Dehler, C.E.; Król, E. Transcriptomic responses in the fish intestine. *Dev. Comp. Immunol.* **2016**, *64*, 103–117. [[CrossRef](#)]
25. Duan, Y.; Wang, Y.; Xiong, D.; Zhang, J. RNA-seq revealed the signatures of immunity and metabolism in the *Litopenaeus vannamei* intestine in response to dietary succinate. *Fish Shellfish Immunol.* **2019**, *95*, 16–24. [[CrossRef](#)]
26. Qiu, W.; Liu, S.; Yang, F.; Dong, P.; Yang, M.; Wong, M.; Zheng, C. Metabolism disruption analysis of zebrafish larvae in response to BPA and BPA analogs based on RNA-Seq technique. *Ecotoxicol. Environ. Saf.* **2019**, *174*, 181–188. [[CrossRef](#)]
27. Li, Y.; Tsim, K.W.-K.; Wang, W.-X. Copper promoting oyster larval growth and settlement: Molecular insights from RNA-seq. *Sci. Total Environ.* **2021**, *784*, 147159. [[CrossRef](#)]

28. Mohsen, M.; Sun, L.; Lin, C.; Huo, D.; Yang, H. Mechanism underlying the toxicity of the microplastic fibre transfer in the sea cucumber *Apostichopus japonicus*. *J. Hazard. Mater.* **2021**, *416*, 125858. [[CrossRef](#)]
29. Hernández-Pérez, J.; Naderi, F.; Chivite, M.; Soengas, J.L.; Míguez, J.M.; López-Patiño, M.A. Influence of Stress on Liver Circadian Physiology. A Study in Rainbow Trout, *Oncorhynchus mykiss*, as Fish Model. *Front. Physiol.* **2019**, *10*, 611. [[CrossRef](#)]
30. Liu, Y.; Jia, X.; Zhu, H.; Zhang, Q.; He, Y.; Shen, Y.; Xu, X.; Li, J. The effects of exposure to microplastics on grass carp (*Ctenopharyngodon idella*) at the physiological, biochemical, and transcriptomic levels. *Chemosphere* **2021**, *286*, 131831. [[CrossRef](#)]
31. Vieira, K.S.; Neto, J.A.B.; Crapez, M.A.C.; Gaylarde, C.; Pierri, B.d.; Saldaña-Serrano, M.; Bainy, A.C.D.; Nogueira, D.J.; Fonseca, E.M. Occurrence of microplastics and heavy metals accumulation in native oysters *Crassostrea Gasar* in the Paranaguá estuarine system, Brazil. *Mar. Pollut. Bull.* **2021**, *166*, 112225. [[CrossRef](#)] [[PubMed](#)]
32. Tse-Lynn, L.; Alexander, T.; Lindsay, A.; Ratanawalee, P. Species in wildlife trade: Socio-economic factors influence seahorse relative abundance in Thailand. *Biol. Conserv.* **2016**, *201*, 301–308.
33. Groten, J.P.; Feron, V.J.; Sühnel, J. Toxicology of simple and complex mixtures. *Trends Pharmacol. Sci.* **2001**, *22*, 316–322. [[CrossRef](#)]
34. Prato, E.; Biantolino, F. Combined toxicity of mercury, copper and cadmium on embryogenesis and early larval stages of the *Mytilus galloprovincialis*. *Environ. Technol.* **2007**, *28*, 915–920. [[CrossRef](#)]
35. Jinhui, S.; Sudong, X.; Yan, N.; Xia, P.; Jiahao, Q.; Yongjian, X. Effects of microplastics and attached heavy metals on growth, immunity, and heavy metal accumulation in the yellow seahorse, *Hippocampus kuda* Bleeker. *Mar. Pollut. Bull.* **2019**, *149*, 110510. [[CrossRef](#)]
36. Brown, R.A.M.; Epis, M.R.; Horsham, J.L.; Kabir, T.D.; Richardson, K.L.; Leedman, P.J. Total RNA extraction from tissues for microRNA and target gene expression analysis: Not all kits are created equal. *BMC Biotechnol.* **2018**, *18*, 1–11. [[CrossRef](#)]
37. Zhao, S. Assessment of the impact of using a reference transcriptome in mapping short RNA-Seq reads. *PLoS ONE* **2014**, *9*, e101374. [[CrossRef](#)]
38. Grabherr, M.G.; Haas, B.J.; Yassour, M.; Levin, J.Z.; Thompson, D.A.; Amit, I.; Adiconis, X.; Fan, L.; Raychowdhury, R.; Zeng, Q.; et al. Full-length transcriptome assembly from RNA-Seq data without a reference genome. *Nat. Biotechnol.* **2011**, *29*, 644–652. [[CrossRef](#)]
39. Alvarez, R.V.; Vidal, N.M.; Garzón-Martínez, G.A.; Barrero, L.S.; Landsman, D.; Mariño-Ramírez, L. Workflow and web application for annotating NCBI BioProject transcriptome data. *Database* **2017**, *2017*, bax008. [[CrossRef](#)]
40. Mortazavi, A.; Williams, B.A.; McCue, K.; Schaeffer, L.; Wold, B. Mapping and quantifying mammalian transcriptomes by RNA-Seq. *Nat. Methods* **2008**, *5*, 621–628. [[CrossRef](#)]
41. Kima, H.; Lee, B.; Han, J.; Lee, Y.H.; Min, G.; Kim, S.; Lee, J. De novo assembly and annotation of the Antarctic copepod (*Tigriopus kingsejongensis*) transcriptome. *Mar. Genom.* **2016**, *28*, 37–39. [[CrossRef](#)] [[PubMed](#)]
42. Li, B.; Dewey, C.N. RSEM: Accurate transcript quantification from RNA-Seq data with or without a reference genome. *BMC Bioinform.* **2011**, *12*, 1–16. [[CrossRef](#)] [[PubMed](#)]
43. Wang, Z.; Gerstein, M.; Snyder, M. RNA-Seq: A revolutionary tool for transcriptomics. *Nat. Rev. Genet.* **2009**, *10*, 57–63. [[CrossRef](#)] [[PubMed](#)]
44. Livak, K.J.; Schmittgen, T.D. Analysis of relative gene expression data using real-time quantitative PCR and the $2^{-\Delta\Delta CT}$ Method. *Methods* **2001**, *25*, 402–408. [[CrossRef](#)]
45. Peixoto, D.; Torreblanca, A.; Pereira, S.; Vieira, M.N.; Varó, I. Effect of short-term exposure to fluorescent red polymer microspheres on *Artemia franciscana* nauplii and juveniles. *Environ. Sci. Pollut. Res.* **2021**, *29*, 6080–6092. [[CrossRef](#)] [[PubMed](#)]
46. Qian, B.; Xue, L. Liver transcriptome sequencing and de novo annotation of the large yellow croaker (*Larimichthys crocea*) under heat and cold stress. *Mar. Genom.* **2016**, *25*, 95–102. [[CrossRef](#)]
47. Wang, S.; Xie, S.; Wang, Z.; Zhang, C.; Pan, Z.; Sun, D.; Xu, G.; Zou, J. Single and Combined Effects of Microplastics and Cadmium on the Cadmium Accumulation and Biochemical and Immunity of *Channa argus*. *Biol. Trace Element Res.* **2021**, *200*, 3377–3387. [[CrossRef](#)]
48. Yuan, W.; Zhou, Y.; Chen, Y.; Liu, X.; Wang, J. Toxicological effects of microplastics and heavy metals on the *Daphnia magna*. *Sci. Total Environ.* **2020**, *746*, 141254. [[CrossRef](#)]
49. Boopathy, L.R.A.; Jacob-Tomas, S.; Alecki, C.; Vera, M. Mechanisms tailoring the expression of heat shock proteins to proteostasis challenges. *J. Biol. Chem.* **2022**, *198*, 101796. [[CrossRef](#)]
50. Dubrez, L.; Causse, S.; Bonan, N.B.; Dumétier, B.; Garrido, C. Heat-shock proteins: Chaperoning DNA repair. *Oncogene* **2020**, *39*, 516–529. [[CrossRef](#)]
51. Farrell, P.; Nelson, K. Trophic level transfer of microplastic: *Mytilus edulis* (L.) to *Carcinus maenas* (L.). *Environ. Pollut.* **2013**, *177*, 1–3. [[CrossRef](#)] [[PubMed](#)]
52. Luís, L.G.; Ferreira, P.; Fonte, E.; Oliveira, M.; Guilhermino, L. Does the presence of microplastics influence the acute toxicity of chromium (VI) to early juveniles of the common goby (*Pomatoschistus microps*)? A study with juveniles from two wild estuarine populations. *Aquat. Toxicol.* **2015**, *164*, 163–174. [[CrossRef](#)] [[PubMed](#)]
53. Mates, J. Effects of antioxidant enzymes in the molecular control of reactive oxygen species toxicology. *Toxicology* **2000**, *153*, 83–104. [[CrossRef](#)]
54. Schülke, S.; Dreidax, D.; Malik, A.; Burmester, T.; Nevo, E.; Band, M.; Avivi, A.; Hankeln, T. Living with stress: Regulation of antioxidant defense genes in the subterranean, hypoxia-tolerant mole rat, *Spalax*. *Gene* **2012**, *500*, 199–206. [[CrossRef](#)]

55. Karimian, A.; Mir, S.M.; Parsian, H.; Refieyan, S.; Mirza-Aghazadeh-Attari, M.; Yousefi, B.; Majidinia, M. Crosstalk between Phosphoinositide 3-kinase/Akt signaling pathway with DNA damage response and oxidative stress in cancer. *J. Cell. Biochem.* **2018**, *120*, 10248–10272. [[CrossRef](#)]
56. Sun, Y.; Zhang, X.; Wang, G.; Lin, S.; Zeng, X.; Wang, Y.; Zhang, Z. PI3K-AKT signaling pathway is involved in hypoxia/thermal-induced immunosuppression of small abalone *Haliotis diversicolor*. *Fish Shellfish Immunol.* **2016**, *59*, 492–508. [[CrossRef](#)]
57. Bottiglione, F.; Dee, C.T.; Lea, R.; Zeef, L.A.H.; Badrock, A.P.; Wane, M.; Bugeon, L.; Dallman, M.J.; Allen, J.E.; Hurlstone, A.F.L. Zebrafish IL-4-like Cytokines and IL-10 Suppress Inflammation but Only IL-10 Is Essential for Gill Homeostasis. *J. Immunol.* **2020**, *205*, 994–1008. [[CrossRef](#)]
58. Baumann, L.; Schmidt-Posthaus, H.; Segner, H.; Wolf, J.C. Comment on “uptake and accumulation of polystyrene microplastics in zebrafish (*Danio rerio*) and toxic effects in liver”. *Environ. Sci. Technol.* **2016**, *50*, 12521–12522. [[CrossRef](#)]
59. Ren, Y.; Ding, D.; Pan, B.; Bu, W. The TLR13-MyD88-NF- κ B signalling pathway of *Cyclina sinensis* plays vital roles in innate immune responses. *Fish Shellfish Immun.* **2017**, *70*, 720–730. [[CrossRef](#)]
60. Nasser, F.; Lynch, I. Secreted protein eco-corona mediates uptake and impacts of polystyrene nanoparticles on *Daphnia magna*. *J. Proteom.* **2016**, *137*, 45–51. [[CrossRef](#)]
61. Li, D.; Yao, H.; Du, L.; Zeng, X.; Xiao, Q. Thallium(I and III) exposure leads to liver damage and disorders of fatty acid metabolism in mice. *Chemosphere* **2022**, *307*, 135618. [[CrossRef](#)] [[PubMed](#)]
62. Campani, T.; Baini, M.; Giannetti, M.; Cancelli, F.; Mancusi, C.; Serena, F.; Marsili, L.; Casini, S.; Fossi, M.C. Presence of plastic debris in loggerhead turtle stranded along the Tuscany coasts of the Pelagos Sanctuary for Mediterranean Marine Mammals (Italy). *Mar. Pollut. Bull.* **2013**, *74*, 225–230. [[CrossRef](#)] [[PubMed](#)]
63. Miller, W.L. Steroidogenic acute regulatory protein (StAR), a novel mitochondrial cholesterol transporter. *Biochim. Biophys. Acta Mol. Cell Res.* **2007**, *1771*, 663–676. [[CrossRef](#)] [[PubMed](#)]
64. Debeljak, N.; Horvat, S.; Vouk, K.; Lee, M.; Rozman, D. Characterization of the Mouse Lanosterol 14 α -Demethylase (CYP51), a New Member of the Evolutionarily Most Conserved Cytochrome P450 Family. *Arch. Biochem. Biophys.* **2000**, *379*, 37–45. [[CrossRef](#)] [[PubMed](#)]
65. Campos, A.; Clemente-Blanco, A. Cell Cycle and DNA Repair Regulation in the Damage Response: Protein Phosphatases Take Over the Reins. *Int. J. Mol. Sci.* **2020**, *21*, 446. [[CrossRef](#)] [[PubMed](#)]